Available online at www.sciencedirect.com

SCIENCE DIRECT®

Journal of volcanology and geothermal research

ELSEVIER

Journal of Volcanology and Geothermal Research 146 (2005) 60–76

www.elsevier.com/locate/jvolgeores

Seismicity and tilt associated with the 2003 Anatahan eruption sequence

Sara H. Pozgay[a,*], Randall A. White[b], Douglas A. Wiens[a], Patrick J. Shore[a], Allan W. Sauter[c], Jose L. Kaipat[d]

[a]*Washington University in St. Louis, St. Louis, MO, United States*
[b]*U.S. Geological Survey, Menlo Park, CA, United States*
[c]*Scripps Institution of Oceanography, La Jolla, CA, United States*
[d]*Emergency Management Office, Saipan, MP, United States*

Received 22 October 2004; accepted 28 December 2004

Abstract

On May 10, 2003, the first historical eruption of Anatahan volcano in the western Pacific Mariana Islands was fortuitously recorded by a broadband seismograph installed on the island only 4 days prior to the eruption. This station, located 7 km WNW of the active crater, together with another broadband seismograph on Sarigan Island 45 km to the north, continued to operate throughout the 2-month period of major eruptive activity in May and June and throughout the majority of the following year. In June 2003, the Saipan Emergency Management Office and the US Geological Survey installed two telemetered high-gain short-period seismic stations to monitor the activity in real-time. The only earthquakes detected in the 4-day period from the initial seismograph installation until 6 h prior to the eruption occurred approximately 20 km to the northeast of the island on May 8. The first volcano-tectonic (VT) event located near the volcano occurred at 01:53 GMT on May 10. The number of events per hour then increased dramatically and a period of about 80 discrete earthquakes per hour commenced at about 06:20 GMT, immediately prior to the estimated eruption time of 07:30 from the Volcanic Ash Advisory Center. A long-period tilt signal recorded on the horizontal components of the broadband seismograph, indicating upward movement of the crater region, also commenced at about 06:20. Inflation continued until 09:30, when the direction of tilt reversed. Deflation continued until 17:50, coinciding with a reduction in the number of VT events. The larger VT events were located with a linearized least-squares location algorithm. Magnitudes of located VT events on May 10 ranged from 2.0 to 3.2, but a period of larger VT events were recorded on May 11, with the largest M 4.2. After about 36 h of intense earthquake activity, the number of discrete VT events declined and was replaced by nearly continuous volcanic tremor for the next 6 weeks. Differing types of very long-period events may suggest complex non-destructive magmatic source mechanisms, persisting dominantly throughout the first 10 days of the initial eruption. Visual reports indicate that a small craggy dome extruded sometime between May 20 and June 5. From analogy with other volcanic dome extrusions, we believe the dome probably extruded just as the tremor amplitude decreased

* Corresponding author. Fax: +1 314 935 7361.
E-mail address: spozgay@wustl.edu (S.H. Pozgay).

0377-0273/$ - see front matter
doi:10.1016/j.jvolgeores.2004.12.008

dramatically about May 24. This dome was then destroyed between June 13 and 14. Reduced displacement of the co-eruption tremor is estimated as approximately 40–80 cm^2, suggesting an eruption with a Volcanic Explosivity Index of about 3.

Keywords: Anatahan; Mariana Islands; volcano seismology; broadband; VLP; tilt

1. Introduction

The first historical eruption of the Anatahan stratovolcano in the western Pacific Mariana island arc on May 10, 2003 was fortuitously recorded by a broadband seismograph installed 7 km WNW of the active crater 4 days prior to the onset of the eruption. The phreatomagmatic eruption was dominated by hot low-viscosity andesite (Pallister et al., 2005—this issue). Eruption-related high-frequency volcano-tectonic (VT) earthquakes, long-period (LP) earthquakes, very long-period (VLP) events, and a tilt signal were accurately recorded by the broadband seismograph. Similar seismic recordings across a wide range of frequencies commencing prior to the initial eruption of a historically inactive volcano have rarely been obtained.

Although local seismic monitoring of Anatahan has been discontinuous, two seismic swarms prior to the 2003 eruption have been reported. A small earthquake swarm occurred between March 31 and April 1, 1990 with events roughly located at varying distances northwest of the island using *S–P* times from nearby WWSSN stations (Banks and Ewert, 1990; Sasamoto et al., 1990). This resulted in the evacuation of inhabitants in early April 1990 and the installation of a USGS telemetered seismograph the following September. The only other documented seismic swarm occurred between May and August of 1993. These earthquakes all had focal depths less than ~10 km and magnitudes less than ~3.0, most less than ~1.5 (Koyanagi and Chong, 1993). People have lived on the island periodically over the past few years and last left in March 2003. There were no reported volcanic events during that time.

Although monitoring was inadequate prior to the May 10, 2003 eruption, no evidence exists for any large-scale precursory activity prior to May 8. Earthquakes with magnitude <~4.5 may have occurred prior to installation of the Anatahan seismograph on May 6, although no earthquakes larger than M ~4.5 have occurred on or near the island in the entire year before the eruption, as they would have been recorded at the IRIS-GSN station on Guam (GUMO) and reported to the National Earthquake Information Center. Government employees from Saipan were on the island from April 14–26, 2003 and camped inside the crater for two evenings. They reported feeling no earthquakes or tremors.

2. Data set

2.1. Previous seismic stations

Due to their remote location, seismological monitoring of the Northern Mariana volcanoes has been intermittent. The WWSSN had one station at the northern end of Guam (GUA), installed in 1962. This station was augmented and ultimately replaced with a digital borehole station (GUMO) in June 1975 (Fig. 1). This station is too distant to monitor all but the largest volcano-associated events. In early 1990, Anatahan inhabitants felt small seismic swarms (Banks and Ewert, 1990; Sasamoto et al., 1990), which prompted the late-September installation of a short-period (1 Hz) vertical-component seismograph on Anatahan (ANAT) with a receiving station at the Emergency Management Office (EMO) in Saipan (Table 1). Data were telemetered back to EMO for real-time analysis. EMO reports that no other significant seismic activity has occurred near the island since the seismic swarm in May–August 1993 (Koyanagi and Chong, 1993). The ANAT seismic station operated approximately 50% of the time between 1990 and 2004, with data gaps caused by a lack of funding and maintenance.

2.2. The Anatahan Broadband Seismograph (ANAH)

Shortly before the May 10 eruption, personnel from Washington University in St. Louis and

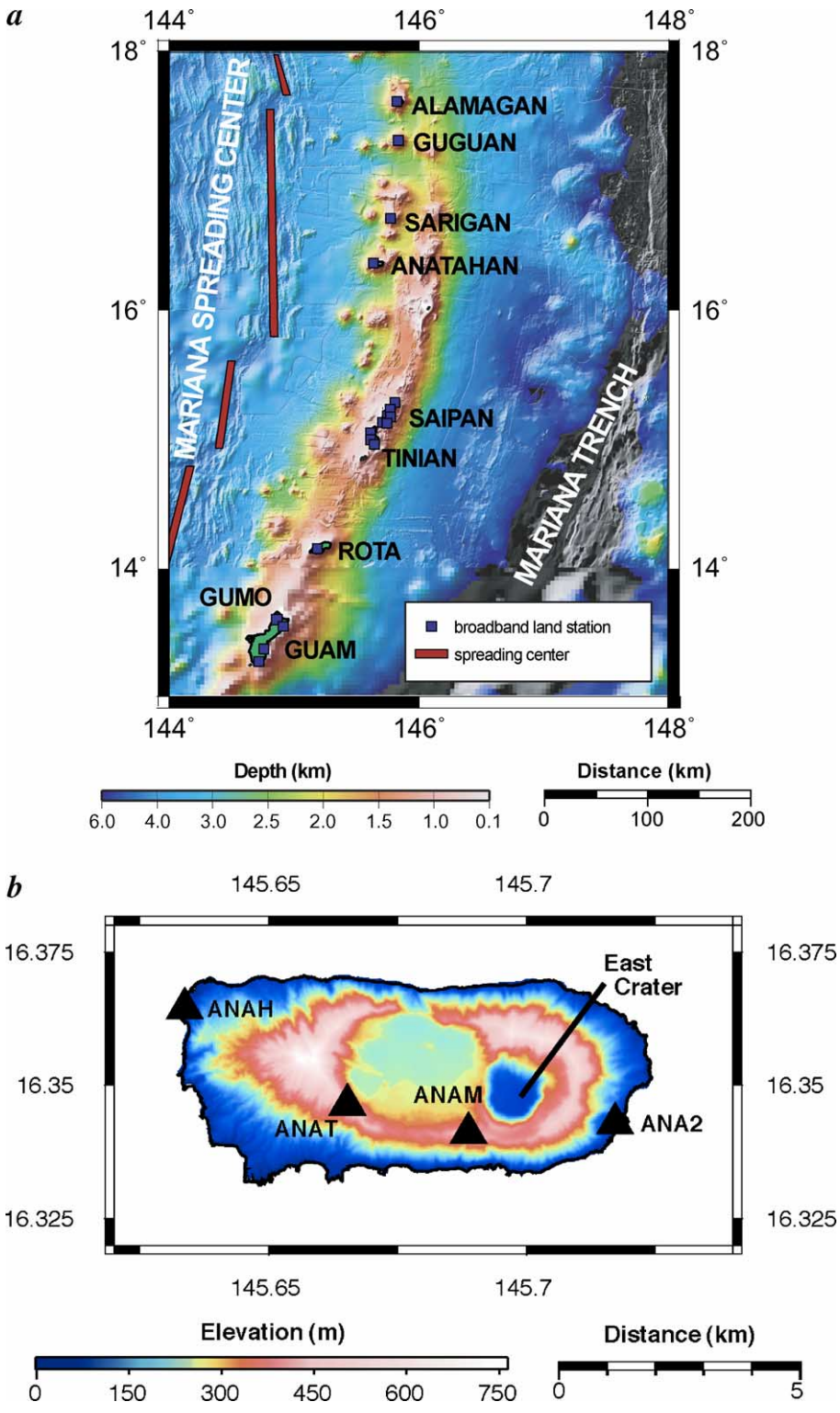
a
144°
146°
148°
18°
16°
14°
ALAMAGAN
GUGUAN
SARIGAN
ANATAHAN
SAIPAN
TINIAN
ROTA
GUMO
GUAM
MARIANA SPREADING CENTER
MARIANA TRENCH
broadband land station
spreading center
Depth (km)
6.0 4.0 3.0 2.5 2.0 1.5 1.0 0.1
Distance (km)
0 100 200
b
145.65
145.7
16.375
16.35
16.325
East Crater
ANAH
ANAM
ANAT
ANA2
Elevation (m)
0 150 300 450 600 750
Distance (km)
0 5

Table 1
Station locations and dates of operation

Station name	Latitude (°)	Longitude (°)	Elevation (m)	Install date	Down time[a]
ANAH[b]	16.3644	145.6337	91	5/6/2003	7/23/03–9/6/03, 4/15/04–4/25/04
ANAT[c]	16.3464	145.6653	531	9/28/1990	~50%
ANA2[d]	16.3429	145.7172	69	6/5/2003	None
ANAM[d]	16.3411	145.6888	484	7/15/2004	None
Sarigan[b]	16.7069	145.7697	85	5/6/2003	None
Guguan[b]	17.3116	145.8334	80	5/7/2003	None
Alamagan[b]	17.6124	145.8214	71	5/8/2003	None
Saipan[e]	15.2340	145.7670	219	5/2/2003	None

[a] Range of days station is off.
[b] PASSCAL STS-2, NSF/Margins Science Group, Washington University in St Louis.
[c] 1-Hz vertical Mark-4, Emergency Management Office, Saipan, MP.
[d] 1-Hz vertical L-4 USGS, Menlo Park, CA.
[e] PASSCAL CMG-40T, NSF/Margins Science Group, Washington University in St Louis.

Scripps Institution of Oceanography installed a network of 20 PASSCAL broadband seismographs on the Mariana Islands. This installation was part of a 1-year US–Japanese project to image the deep seismic structure of the Mariana arc and was funded by the MARGINS program of the National Science Foundation (Fig. 1a). The seismograph installation team was among the first to observe the ~4-km-high ash plume while sailing past the island on the *Super Emerald* early on the morning of May 11. The STS-2 seismograph at Anatahan (ANAH) (Fig. 1b) was placed on a prefabricated concrete slab cemented to the existing hard clay approximately 1 m below the surface. The sensor was protected from flooding and thermal variations with a 15-gallon plastic drum and layers of styrofoam. A 55-gallon barrel enclosed the sensor vault, and the entire unit was buried. Data were logged by a Reftek 72–08 recorder at 40 sps, giving the system a bandpass from 0.008–18 Hz. ANAH operated from its installation on May 6, 2003 at 06:00 GMT to August 14, 2004, with power outages from July 23, 2003 through September 6, 2003 and April 15 to April 25, 2004, most likely due to ash on the solar panels from minor eruptions (Table 1).

2.3. USGS/EMO Installations of ANA2, ANAT, and ANAM

On June 5, 2003, the US Geological Survey and the Emergency Management Office installed a short-period vertical-component seismograph (ANA2) on the eastern end of the island about 1 km from the active vent (Table 1, Fig. 1b). The telemetered short-period vertical station (ANAT) was brought up and running near the middle of the island later that month. At least one of these two stations was operating continuously during 2003 and were monitored in real-time by personnel from EMO and USGS. In July 2004, the USGS and EMO installed a third telemetered short-period vertical station (ANAM) near the western crater rim. At the same time, two microphones were also installed, co-located with seismic stations ANAM and ANAT.

3. Observations

3.1. Event classification

The Anatahan broadband station recorded a variety of volcanic signals during the initial eruption sequence (Fig. 2). The high-frequency volcano-

Fig. 1. (a) Bathymetric map of the Mariana island arc showing the location of Anatahan relative to the other islands. Blue squares show broadband seismograph stations installed as part of the Mariana Subduction Factory Imaging Experiment. (b) Seismic stations at Anatahan Island. Topography is courtesy of Steve Schilling (NOAA) and island contour from Bill Chadwick (NOAA). (For interpretation of the references to colour in this figure legend, the reader is referred to the web version of this article.)

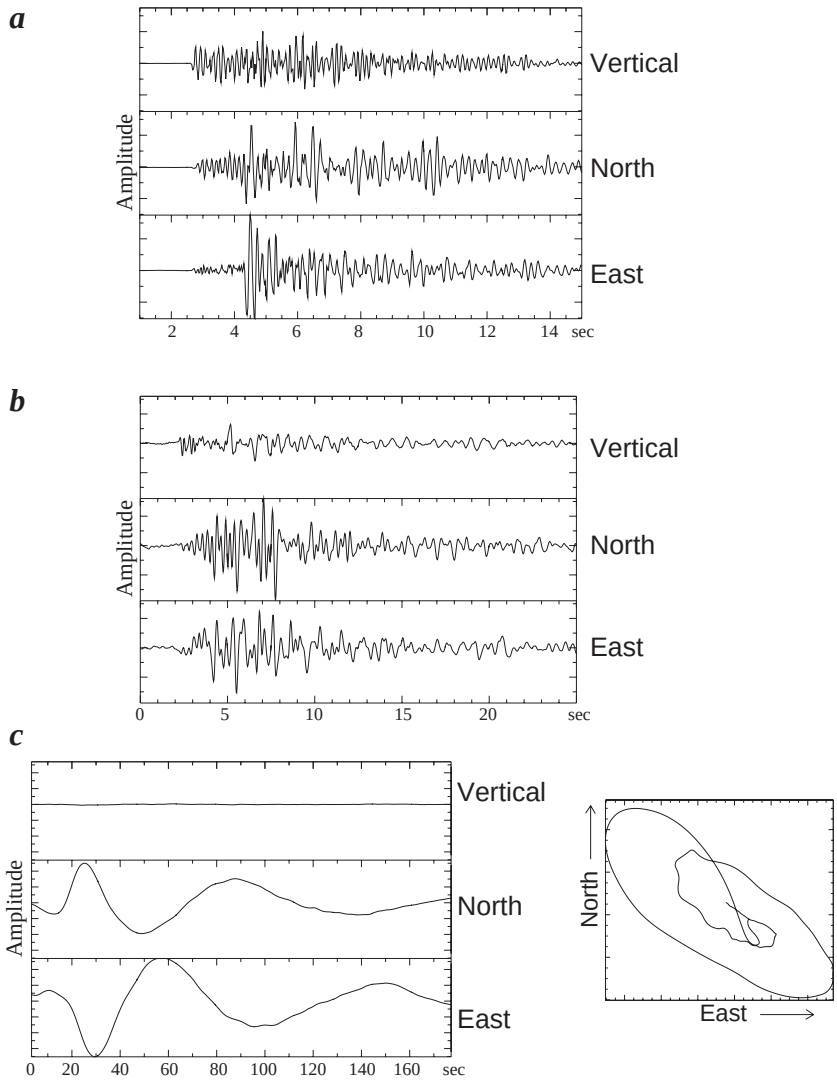

Fig. 2. Typical seismic recordings at the Anatahan broadband station. Each event is auto-scaled to the largest component. (a) Volcano-tectonic (VT) event on May 10 at 04:51 GMT. (b) Long-period (LP) event on May 14 at 11:26 GMT. (c) Left: very long-period (VLP) event on May 18 at 08:48 GMT, filtered with a passband from 14–100 s. (c) Right: horizontal particle motion for VLP event, with North motion upward and East towards the right. Each figure shows the vertical component seismogram on top, N–S in the middle, and E–W at the bottom.

tectonic (VT) events exhibit frequencies of ~5 Hz and characteristic *S*–*P* times of 1.5–2.5 s (Fig. 2a). The larger VT events were generally recorded at the nearby seismograph on Sarigan Island. VT events with magnitudes larger than ~3.5 were also recorded at Guguan, Alamagan, and Saipan.

In addition to VT events, we observed long-period (LP) events and very long-period (VLP) events. The LP events are characterized by frequencies of <~4–5 Hz, strong *P* arrivals, and emergent *S* arrivals (Fig. 2b). Typically, LP events begin with a higher frequency component (3–5 Hz) superimposed upon the dominant frequency and lasting for 1–1.5 s. Earthquake locations could not be computed for the LP events due to the emergent *S* phases, but they are typically located in the upper kilometer or so beneath active craters (Chouet, 2003 ; Lahr et al., 1994; Rowe et al., 2004). Deeper LP earthquakes typically have clearly defined *S* arrivals, lack surface waves, and would probably have been recorded at Sarigan Island, all of which are contrary to

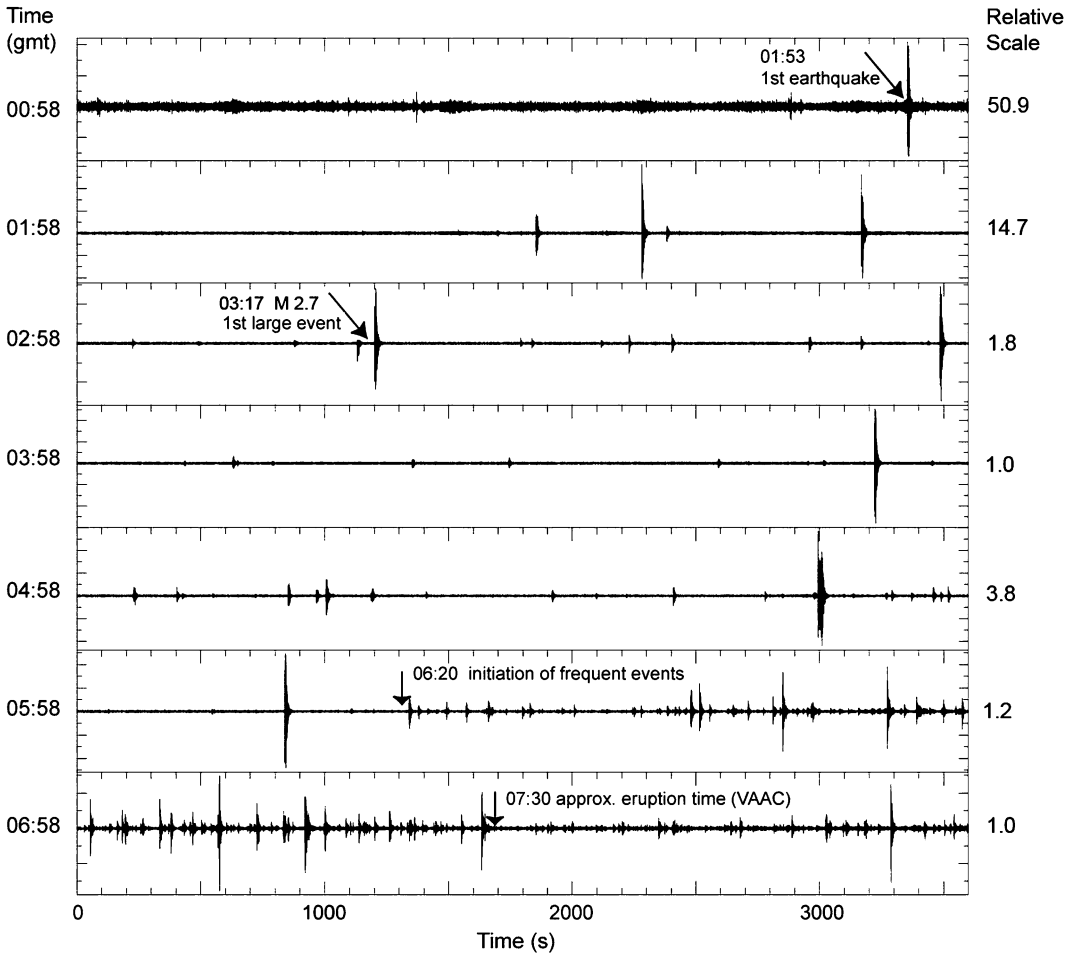

Fig. 3. Six-hour record of the initial onset of the eruption on May 10, 2003 recorded by the broadband seismograph on Anatahan. Each trace is 1 h of data on the vertical component. Each trace is auto-scaled to largest event, with the relative scaling factor indicated at the right.

this eruption record. The VLP events have typical periods of 25–>50 s and are characterized by a single or double pulse waveform (Fig. 2c). Observed VLP signals are dominant on the horizontal components and nearly absent on the vertical, suggesting source locations at approximately the same elevation as ANAH. Fig. 2c shows a typical VLP event with a 14–100-s band-pass filter applied and the horizontal particle motion, showing a rough azimuth to the event. These events may be observed in the raw data (see later section).

We observed moderately large amplitude long-period volcanic tremor beginning May 10 lasting until May 24, then low amplitude tremor through June 24. The tremor is comprised of LP event signals that are so frequent as to be severely overlapping.

3.2. Chronology

Only two earthquakes were detected in the 4-day period from the seismograph installation on May 6 until a few hours before the eruption. Both occurred on May 8 and were located approximately 20 km northeast of the island near a large seamount. Although not certain, we believe these events are related to the eruption process and we refer to them as distal VTs (White and Power, 2001). Such distal VTs have often been observed preceding eruptions at distances of 2 to more than 20 km or further from the eruptive center (Almendros et al., 2002; Arciniega-Ceballos et al., 2003; Harlow et al., 1996; White and Power, 2001).

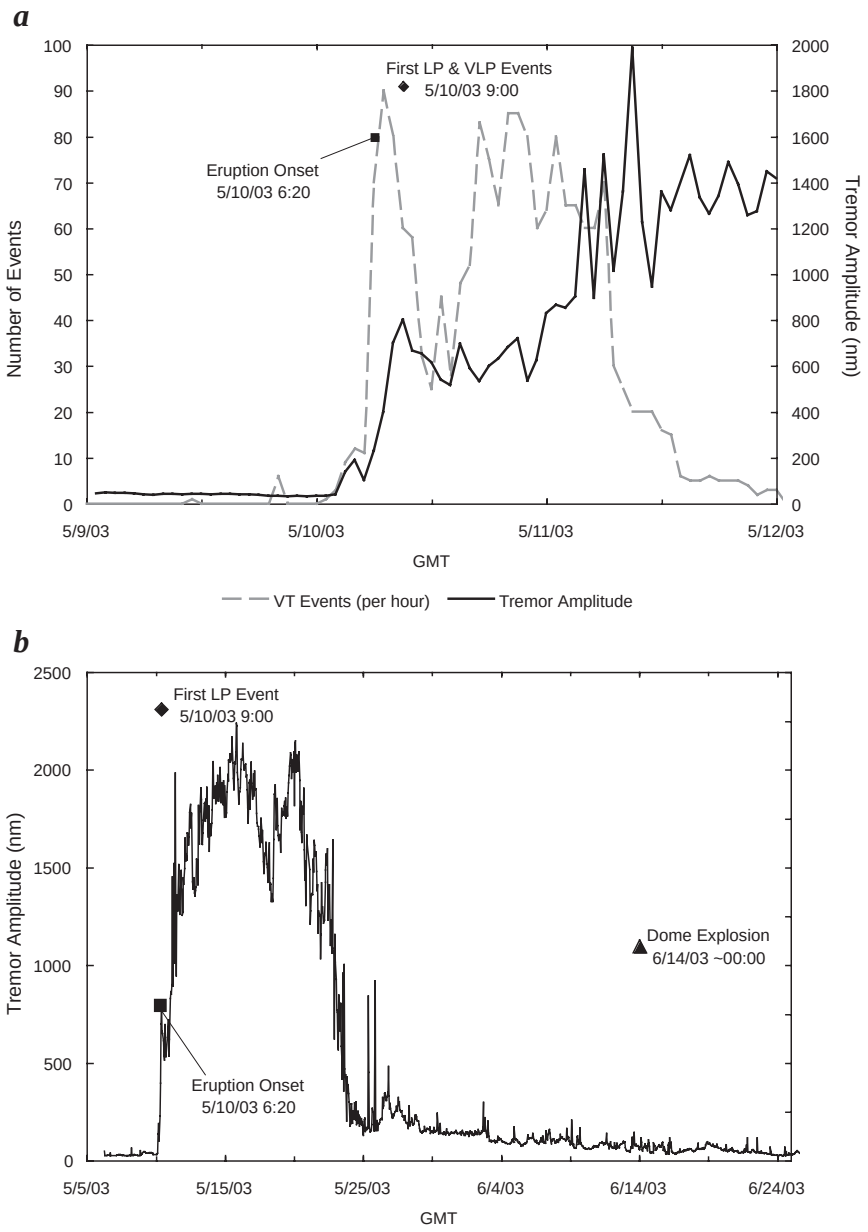

Fig. 4. (a) Handpicked event count (gray dashed) and the tremor amplitude (black solid) for May 9–12. (b) Tremor amplitude for May 5 through June 25. The time of significant events is indicated. See text for discussion.

The first precursory VT event on May 10 occurred at 01:53 GMT[1] (Fig. 3), followed by the first large located VT at 03:17 (magnitude 2.7). The high-frequency volcano-tectonic (VT) event rate increased dramatically to over 80 events per hour at about 06:20, as determined by manually counting the number of discrete identifiable VT arrivals at the broadband Anatahan station (Fig. 4). The exact time of eruption is unknown, as there were no visual reports, but the Volcanic Ash Advisory Center

[1] All times reported in GMT, unless otherwise noted.

(VAAC) estimates the eruption time at 07:30 GMT (Guffanti et al., 2005—this issue). Initial events were all VTs, with the first LP event observed at ~09:00 and VLP events observed soon after. The number of VT events reached a maximum at around 07:00–08:00, then decreased between 10:00 and 16:00, before increasing again and remaining high until 06:00 on May 11. This coincides well with the tilt signal recorded on the broadband seismograph showing inflation of the summit from 06:30–09:30 and deflation from 09:30–14:00 (see later section). The maximum size of individual VT events increased towards the end of this sequence on May 11, with the largest at 13:58 (M 4.07). The volcano was first documented and photographed by the seismograph installation team aboard a small ship at about 19:00 on May 10 (Wiens et al., 2004).

We developed a procedure for tracking the amplitude of the tremor as a function of time. Hour-long velocity-seismograms from the vertical component of ANAH station were bandpass filtered between 0.5 and 5 Hz. Then the average spectral power over this band was calculated using the maximum entropy method (Makhoul, 1975). We averaged and normalized the tremor estimates and plotted the amplitude spectrum (square root of the power spectrum) (Fig. 4). Before running this algorithm, several of the larger earthquakes were manually removed from the data set.

Tremor amplitude increased to ~15–20 times higher than the background noise within the first ~3 h of the eruption (Fig. 4a). This level remained roughly constant for about 18 h, further increasing to approximately 30–50 times the background noise throughout May 11. The significant rise in tremor amplitude is coincident with the decline in the number of VTs per hour and the increase in VT magnitude, particularly during the latter half of May 11 (Fig. 4). Around 20:00 on May 15, tremor amplitudes reached up to a maximum of ~2300 nm (up to 60 times the non-eruptive background noise).

Overall, the spectral power estimates show that the activity was greatest between May 11 and May 22, immediately following the initial May 10 eruption. The drastic decrease in tremor amplitude on May 22–23 corresponds well with the extrusion of a small craggy dome. Visual reports indicate the dome was not visible until June 5 and was destroyed on June 14, corresponding almost certainly with a large explosion seismic signal just before midnight of the preceding evening.

Long-period (LP) events began at 09:00 on May 10, just after the onset of the initial eruption. The first LP events were small, with approximate magnitudes less than M 1 and Reduced Displacements (Dr) less than 10 cm^2. LP tremor amplitude increased dramatically just prior to these LP events, then decreased for about 12 h before increasing greatly and peaking on May 15–16 and again on May 20. The reduced displacements calculated from the largest LP events observed at Sarigan was 40–80 cm^2 and individual LP events during May 10–20 never exceeded M 2.5. This tremor value corresponds to a Volcanic Explosivity Index (VEI) (McNutt, 1994) value of about 3–4, consistent with the initial eruption column height (VEI 3–4). VEI 2–3 is more in keeping with the erupted volume of the initial phase, as reported by Trusdell et al. (2005—this issue). We also observe very long-period (VLP) events in the eruption sequence and will provide a comprehensive analysis in future work.

EMO and Margins personnel visited the island on May 20 and did not see a dome within the active crater. Remote sensing data in the first couple of days of June indicate that the craggy dome had extruded by that time. From analogy with Mt. Pinatubo (Harlow et al., 1996), Montserrat (Rowe et al., 2004), and Guagua Pichincha (Legrand et al., 2002), the dome likely extruded just as the LP seismicity dropped sharply, about May 24.

On June 13 and 14, two explosions occurred which destroyed the small craggy dome. The first explosion was preceded by two VTs; the largest was M 2.6, and two LP events of about M 2.5, or Dr 40–80 cm^2. The explosion was followed by a couple of hours of low amplitude tremor. The second explosion was preceded by two LP events of about M 2.5 and Dr 40–80 cm^2 and followed again by a few hours of tremor. This tremor value for June activity corresponds to a VEI value of 2–3, in keeping with the erupted volume of that dome destruction phase, as reported by Trusdell et al. (2005—this issue).

3.3. Earthquake locations and magnitudes

Approximate earthquake locations were obtained with a linearized least-squares algorithm using the module *dbgenloc* within the Antelope database pro-

gram. We used *P* and *S* arrivals and an island arc velocity model based on the Izu–Bonin arc at ~32°N (Suyehiro et al., 1996). We computed all locations with at least four arrival times from a minimum of two different stations. *P* and *S* arrival times from the broadband seismographs at Sarigan, Guguan, Alamagan, and Saipan were utilized where possible for the large events. We also attempted to use azimuthal data for *P* arrivals calculated from three-component particle motions in an attempt to increase the constraints on earthquake location; however, the azi-

Table 2
Earthquake locations and magnitudes[a]

Date	Origin time[b]	Latitude (°)	Longitude (°)	M[c]	Major (km)[d]	Minor (km)[d]	Strike (deg)[d]	Origin time (+/− s)	Phases[e]
5/8/03	12:11:12.37	16.50	145.79	2.5	1.27	0.16	296.5	0.3	4
5/8/03	13:03:44.35	16.50	145.79	2.5	2.43	0.24	291.7	1.1	4
5/10/03	3:17:43.28	16.33	145.67	2.7	1.05	0.35	334.1	0.2	4
5/10/03	3:55:43.96	16.35	145.66	2.7	1.29	0.27	318.0	0.3	4
5/10/03	4:51:20.42	16.32	145.68	3.3	0.77	0.36	338.6	0.1	4
5/10/03	6:11:40.68	16.33	145.67	3.0	0.52	0.25	328.2	0.1	4
5/10/03	7:13:02.35	16.34	145.67	2.8	1.91	0.46	319.4	0.7	4
5/10/03	8:31:32.62	16.32	145.68	2.9	0.47	0.20	341.3	0.0	4
5/10/03	10:42:31.10	16.33	145.73	2.9	1.89	0.18	334.5	0.7	4
5/10/03	13:37:53.77	16.33	145.66	3.0	2.11	0.30	335.7	0.9	4
5/10/03	21:24:02.80	16.26	145.67	3.2	1.80	0.58	241.0	0.0	4
5/10/03	22:53:00.31	16.38	145.66	2.4	6.68	0.48	299.3	8.5	4
5/11/03	2:01:29.81	16.36	145.69	2.7	3.05	0.14	315.8	1.8	4
5/11/03	2:03:32.44	16.28	145.70	3.4	1.67	0.27	354.8	0.5	4
5/11/03	2:10:29.24	16.36	145.72	2.9	1.60	0.26	313.4	0.5	4
5/11/03	4:03:33.75	16.37	145.69	3.6	1.40	0.24	312.5	0.4	8
5/11/03	4:15:21.22	16.38	145.69	2.8	4.17	0.13	310.1	3.3	4
5/11/03	4:45:27.15	16.39	145.66	2.9	5.74	0.24	305.1	6.3	4
5/11/03	4:56:31.08	16.31	145.72	3.9	1.26	0.54	342.1	0.3	8
5/11/03	5:31:47.17	16.37	145.70	3.1	2.95	0.37	319.5	1.7	4
5/11/03	6:23:17.59	16.32	145.70	3.7	0.99	0.32	354.0	0.2	8
5/11/03	6:57:20.00	16.38	145.70	3.5	1.56	0.20	315.2	0.5	6
5/11/03	7:58:08.63	16.38	145.70	2.9	0.75	0.13	307.5	0.1	4
5/11/03	8:21:15.79	16.37	145.70	3.0	1.97	0.27	313.1	0.7	4
5/11/03	8:34:29.07	16.37	145.71	3.6	0.73	0.12	313.1	0.1	6
5/11/03	8:44:06.99	16.38	145.69	3.2	1.24	0.14	316.2	0.3	4
5/11/03	9:05:47.03	16.36	145.71	3.7	0.74	0.38	328.1	0.1	9
5/11/03	10:10:30.82	16.35	145.70	3.8	0.32	0.23	307.5	0.0	9
5/11/03	10:45:32.85	16.37	145.75	3.2	0.87	0.17	317.5	0.2	6
5/11/03	11:00:48.99	16.37	145.71	3.0	0.89	0.16	311.4	0.2	4
5/11/03	12:15:21.86	16.39	145.70	3.5	1.15	0.16	310.5	0.3	4
5/11/03	13:58:43.55	16.36	145.71	4.1	0.48	0.21	325.3	0.0	9
5/11/03	16:32:33.42	16.28	145.67	3.2	1.63	0.34	6.0	0.5	4
5/11/03	17:46:26.35	16.38	145.69	2.7	2.85	0.13	310.6	1.6	4
5/11/03	19:55:10.39	16.37	145.71	3.1	0.99	0.20	309.4	0.2	4
5/11/03	20:13:43.37	16.28	145.70	3.6	0.78	0.37	352.3	0.1	4
5/12/03	0:48:01.84	16.25	145.61	3.6	1.87	0.56	280.8	0.0	4
5/12/03	9:33:21.55	16.44	145.79	3.0	3.81	0.52	302.5	2.8	4
6/13/03	6:03:51.07	16.44	145.80	2.6	2.73	0.12	299.3	1.4	5
6/15/03	10:44:58.06	16.44	145.79	2.4	1.56	0.26	296.3	0.5	4

[a] All depths fixed at 8.0 km. See text for discussion.
[b] All times in GMT, hh:mm:ss.ss.
[c] Local magnitude.
[d] Semi-major axis, semi-minor axis, and strike of error ellipse.
[e] Number of phases used in location analysis.

muths obtained from particle motions did not yield consistent results. Some locations in June 2003 used arrival time information from ANA2; however, additional uncertainties were introduced because picks from the ANA2 paper records lack the timing precision of the digital station picks.

Initially, the location procedure was allowed to solve for the earthquake depth; these depths ranged from 1 to 12 km. Because of the small number of arrival times for each event and poor constraints on the local seismic velocity structure, the depths were relatively unstable and resulted in scattered geographic locations for the earthquakes. Therefore, the earthquakes were located with the depth fixed. Trials with several different fixed depths between 2 and 12 km yielded the smallest travel time residuals for a depth of 8 km, so all earthquakes were located with depth fixed to that value. The resulting earthquake locations are shown in Table 2. The nominal $1-\sigma$ epicentral uncertainty median values are 1.6 km for the semimajor error ellipse axis and 0.3 km for the semiminor axis; however, the actual uncertainties are considerably larger due to the necessity of fixing the epicentral depth. Realistically, these locations mostly serve to delineate earthquakes near the volcano from distal earthquakes located >~10 km away.

Fig. 5 shows earthquake locations for the first few days of the eruption sequence (Table 2). The east–west scatter in earthquake locations may be caused by the predominant north–south alignment of the recording stations. Fig. 5a shows earthquakes recorded at ANAH and Sarigan (diamonds) separate from larger events recorded at additional stations (circles). Typically, earthquakes on May 10 were too small to be recorded at stations other than ANAH and Sarigan (Fig. 5b). On May 12, activity near the crater largely ceased and the only two events are located at greater distances from the crater. Also, note a significant number of distal VTs located near the northeastern seamount occurring on May 8 and 12 and in June.

We calculated local magnitude for all located VT earthquakes (Fig. 6, Table 2). For the larger events, we

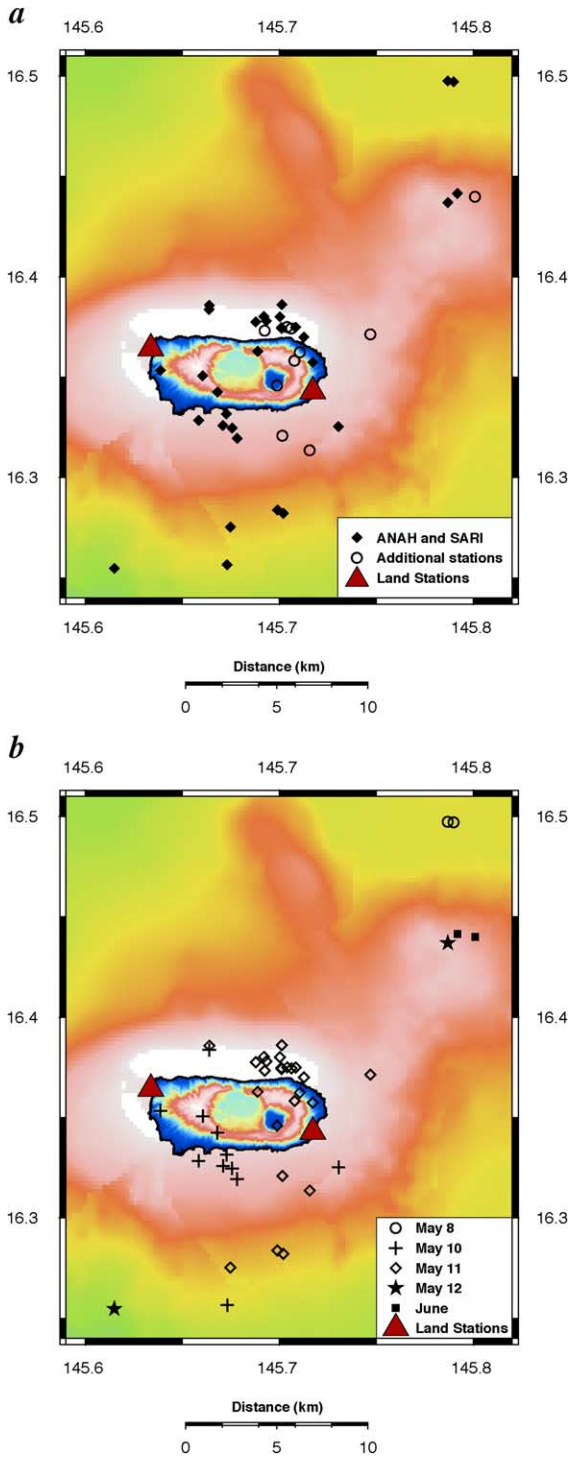

Fig. 5. Maps showing earthquake locations determined from *P* and *S* arrivals with the depths fixed at 8 km. (a) Locations with arrivals from only ANAH and Sarigan are shown as diamonds, locations with any additional stations are shown as circles. (b) Locations plotted as a function of day. Bathymetry and topography scales are same as in Fig. 1. Distance scale is the same for panels a and b.

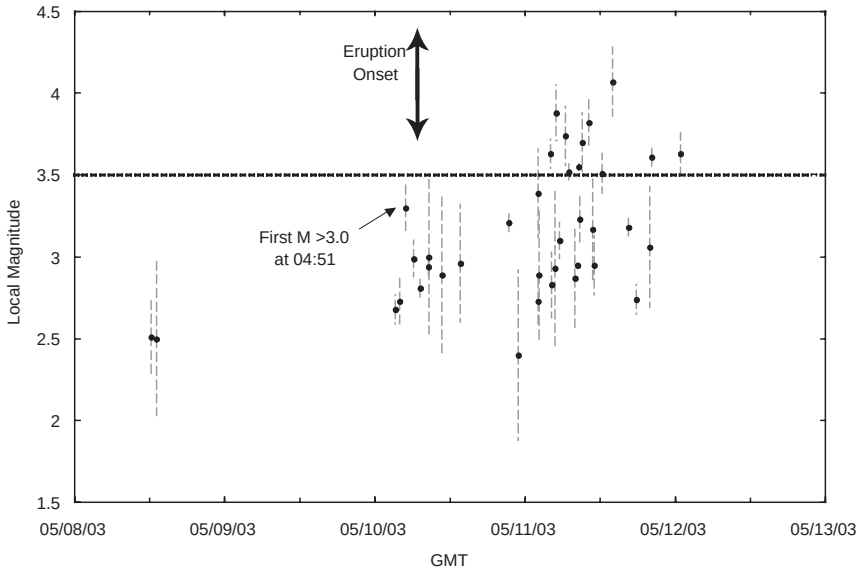

Fig. 6. Magnitude vs. GMT time for earthquakes shown in Fig. 5. Double arrow indicates eruption onset. Single arrow points to first M>3.0 event. Dashed line separates magnitudes at 3.5.

were able to utilize data from other stations, including Guguan, Alamagan, and Saipan. All 25 VT events with M>~3.0 occurred between 04:50 May 10 and 09:34 May 12. Nine VT events with M>3.5 occurred during the interval from 04:00 to 14:00 May 11, with the largest event, M 4.1, occurring at the end of this interval.

3.4. Very long-period events

Two types of VLP events are observed throughout the initial eruption and into mid-June (Fig. 7). Type *A* events have a double-pulse waveform shape with upward first motions, whereas type *B* VLPs exhibit single-pulse waveforms with downward first motions. Both VLP types show two varieties with different dominant periods. Shorter period types show 10–12 s signals (type *A1* and *B1*) and longer period varieties exhibit 30–40 s signals (type *A2* and *B2*). All types of VLPs are observed throughout the May eruption. Type *B2* events dominate the April 2004 eruption (White et al., in preparation).

Type *A1* and *B1* VLP events all occur in association with LP events. Typically, the VLP onset is after the *P* arrival for a given LP event. Type *A2* and *B2* events all occur as distinct VLP sources with no associated higher frequency event. All type *A2* and some type *B2* events are clearly visible in the raw data. The type *B2* events not clearly visible in the raw data are typically associated with small high-frequency events.

Significant similarity of waveform shape for both types of VLP events is suggestive of multiple non-destructive sources. Movement of magmatic sources is the common explanation for such VLP signals (Almendros et al., 2002; Chouet, 1996; Chouet, 2003). Downward first motions may be attributed to an ascending gas bubble or to a contraction at the source, while upward first motions might indicate an expansion at the source. Chouet (2003) observes periodic VLP events coinciding with LP events due to recurrent sill depressurization episodes.

Although several studies have reported one type of VLP event during eruptions, few have VLP signals from the initial eruptive phase of a volcano that has not erupted in more than a century and few have documented four types of VLP signals during an eruption. Almendros et al. (2002) show VLP source depths at approximately 1 and 8 km beneath the Kilauea caldera floor. Although the frequency remained nearly the same between the two sources, VLPs originating at greater depth exhibited simpler waveform shapes than those for shallower depth sources. Another study shows different types of VLP signals at Popocatepetl volcano. The first type results from a shallow source coincident with LP

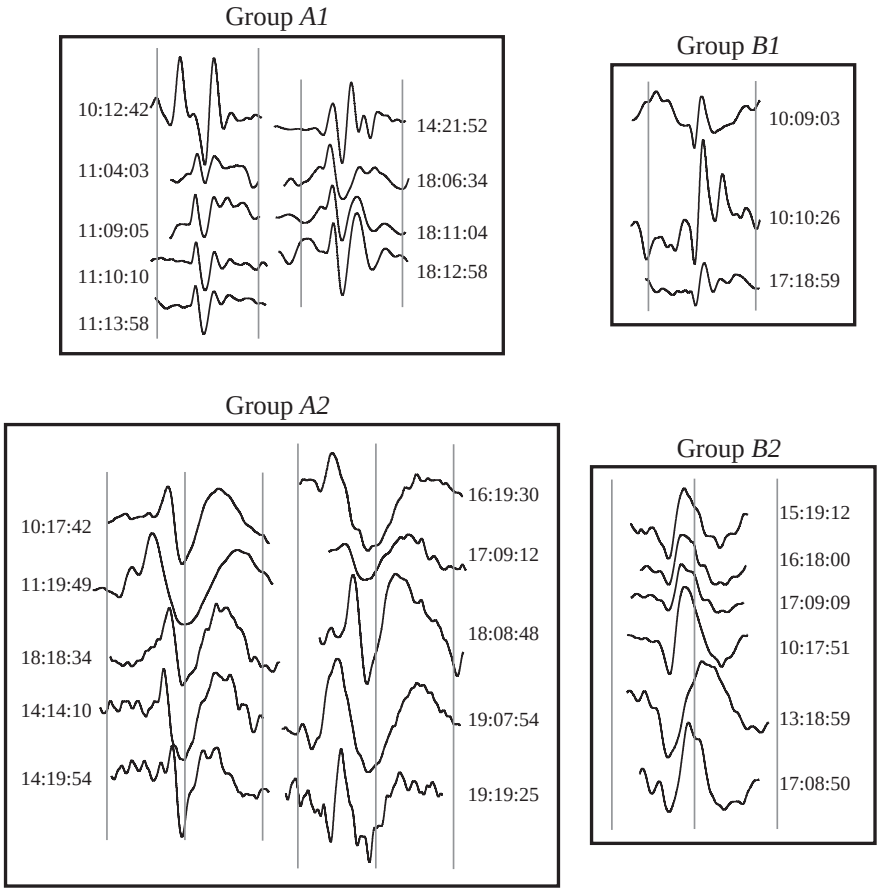

Fig. 7. Very long-period signals from the east–west component broadband station at ANAH. Types *A* and *B* have two dominant frequencies each, 10–12 s (*A1* and *B1*) and 30–40 s (*A2* and *B2*). Scale is the same for each type. All tick marks are separated by 60 s. Waveforms are filtered with a passband from 14–100 s.

source seismicity, while the other source is attributed to a deeper source and linked to monochromatic tremor sequences (Arciniega-Ceballos et al., 2003).

A mechanism to explain differing VLP first motions has not yet been well documented. One viable hypothesis for our observations could include a gas–piston mechanism. This would result in an upward first motion for a deep source, whereas the same mechanism at shallower depths would generate a downward first motion. Another possible hypothesis could be caused by pressure migration, where the vertical dimension of a bubble varies with depth while the horizontal dimension remains constant. Subsequent analysis on the variability of first motions and frequency of observed VLPs will be enlarged upon in a forthcoming study.

3.5. Tilt

Although the STS-2 seismograph is a ground velocity transducer, tilt changes the way the acceleration of gravity affects the horizontal components and thus contributes to the output signal (Rodgers, 1968). The tilt can be obtained from $\Theta(t)=a(t)/\mathbf{g}$, where $a(t)$ is the apparent ground acceleration as recorded by the seismograph and $\mathbf{g}$ is the acceleration due to gravity. In general, the output of a horizontal component broadband seismograph is dominated by ground displacement at short periods (<100 s), but tilt becomes a significant part of the signal at longer periods (Wielandt and Forbriger, 1999). The tilt signal is not recorded on the vertical component, which facilitates discrimination of tilt

signals from ground displacement. Several volcanological studies have observed tilt from broadband seismographs at shorter periods (10–100 s) where it is mixed with the displacement signal (Aster et al., 2003; Chouet et al., 2003; Ohminato et al., 1998). Also, long-period tilt has been recorded by observatory broadband installations (STS-1 seismographs) in Hawaii and Reunion (Ohminato et al., 1998; Battaglia et al., 2000), but there have been no previous tilt studies with portable broadband seismographs.

Beginning at about 06:20 May 10, an extremely long-period signal was recorded on the low-pass filtered EW component seismograph, which is oriented nearly radially from the crater (Figs. 8 and 9). Although it is rare to record an identifiable tilt signal on a portable broadband seismograph, the timing and characteristics of the observed long-period signal strongly indicate a tilt source. The large excursion in the signal begins just at the eruption onset and exceeds the normal diurnal variation (probably due to thermal effects) by a factor of six (Fig. 8). No similar signals are found in the ANAH seismograms at any other time. The absence of any signal on the vertical component and the low amplitude of the signal on the NS component

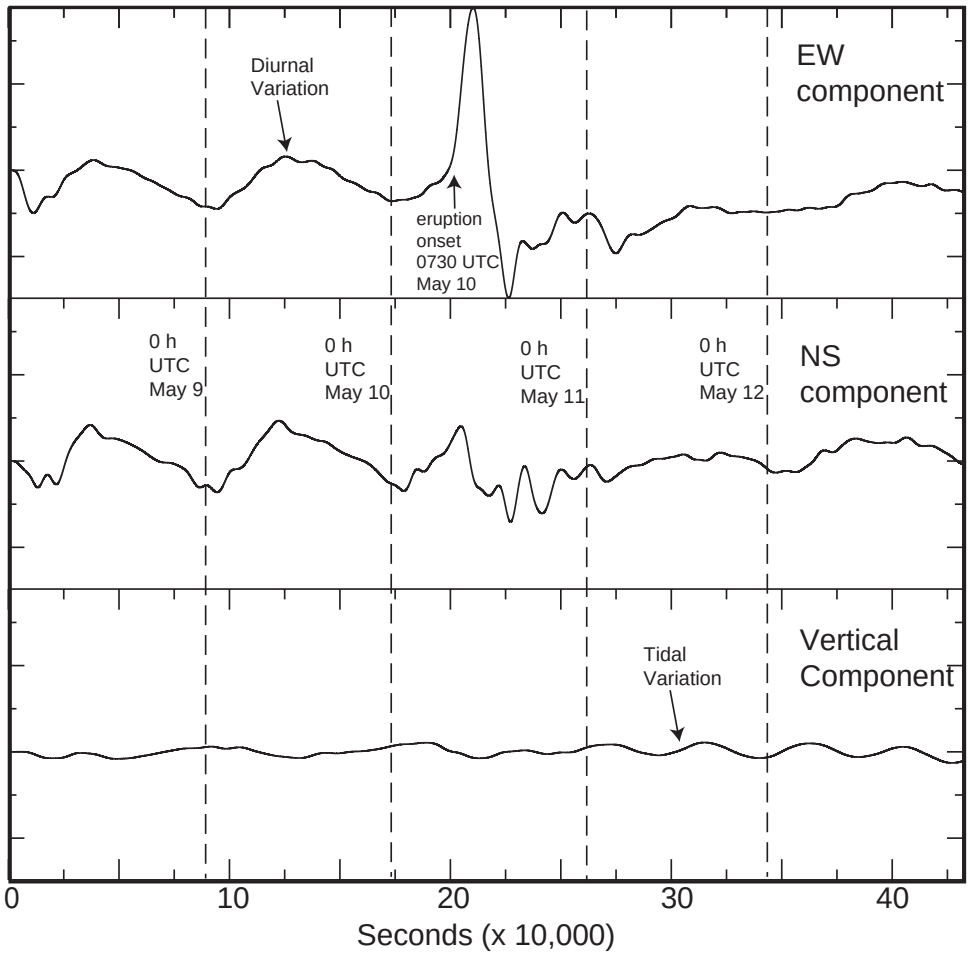

Fig. 8. Seismograms from the Anatahan broadband station for the 5-day period surrounding the eruption. The signals have been low-pass filtered with a corner at 0.001 Hz. The strong signal on the E–W component coincides with the eruption time and is absent on the vertical component and weak on the N–S component, suggesting it results from tilt radial to the crater. The diurnal signal on the horizontal components probably results from minor tilt in response to daily temperature changes, and a tidal signal is also visible on the vertical component.

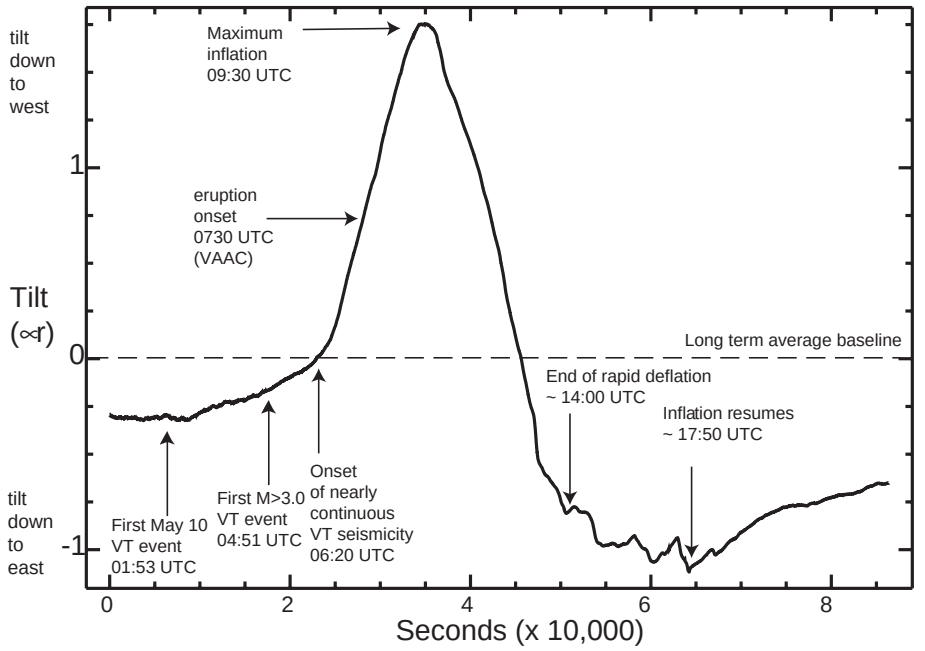

Fig. 9. East–west tilt determined from the Anatahan seismograph for May 10 by deconvolving the E–W record to acceleration and dividing by **g** within a passband from 500–50,000 s. The time of significant events in the sequence is indicated by arrows.

suggest the signal results from tilt along an EW axis, or radial to the crater (Fig. 8).

We processed the records by deconvolving the instrument to obtain apparent acceleration within a bandpass of 500 s to 50,000 s and then divided by **g** to obtain tilt (Fig. 9). As shown in Fig. 9, the onset of the large-scale tilt occurred at about 06:20, coincident with the onset of the highest rate of VT seismicity (Figs. 3 and 4). The sense of this initial tilt is downward to the west, suggesting uplift of the center of Anatahan Island and inflation of the volcano immediately prior to the estimated eruption time of 07:30. Maximum inflation occurred at 09:30, after which rapid deflation occurs until 14:00, coincident with a temporary lull in the occurrence of VT events. After this large-scale deflation, there is some suggestion of a second minor episode of inflation at about 17:00, concurrent with the resumption of VT activity.

Although the broadband seismograph is not sensitive to a DC offset, the amount of deflation on May 10 exceeds the amount of inflation, suggesting some long-term precursory inflation of the crater region may have been relieved during the initial eruption. A geodetic survey suggests that indeed considerable subsidence occurred near the seismic station between January and July, 2003 (Watanabe et al., 2005—this issue). However, this study places the locus of subsidence beneath the station, which is incompatible with the tilt signal since the tilt requires a source eastward of the station near the crater region.

The total magnitude of the initial tilt is about 2 microradians away from the volcanic center, followed by three microradians of tilt towards the crater. One difficulty is that the dominant period of the tilt signal, approximately 25,000 s, is far outside the passband of the instrument, resulting in some instability in the deconvolution process that may result in uncertainty in the tilt magnitude. However, a simple calculation assuming a spherical volume source (Mogi model) shows that the derived tilt magnitude corresponds to an injection volume of 2 million cubic meters assuming a source at optimum depth (4 km) beneath the crater (Wiens et al., submitted for publication). This compares favorably with a total eruption volume (solid rock equivalent) of 10 million cubic meters estimated from ash mapping (Pallister et al., 2005—this issue; Trusdell et al., 2005—this issue) suggesting that the estimated tilt from the seismic records is approximately correct.

4. Discussion

One of the interesting aspects of the 2003 Anatahan eruption is the lack of significant precursory activity before about 6 h prior to the eruption, although some uncertainty remains because significant monitoring began only 4 days prior to the eruption. The only earthquakes recorded within 4 days prior to the sequence were two distal earthquakes about 20 km towards the northeast on May 8. This occurrence of distal earthquakes at distances of even 10s of km from a volcano prior to an initial eruption has been observed previously. These distal VTs generally drop off rapidly in number and size as soon as significant eruptive activity begins. No activity directly associated with the volcano was detected prior to 6 h before the eruption. It is impossible to determine whether there would have been sufficient precursory activity to warn of the impending eruption if a seismic station on Anatahan had been working throughout the year leading up to the eruption.

We assert that the eruption began small and grew slowly based on the total absence of any observable explosion signal anywhere near the time of the onset of the initial phase. The initial eruptive phase is comprised of two intrusive pulses on May 10, the first of which included the first peak in VT activity, the inflationary tilt peak, and the initial LP signals. The second smaller pulse of inflation and the second peak in VT activity followed at about 17:00. The eruption increased in size over the first day or so. VT magnitudes continued to increase past mid-day May 11 and LP tremor amplitudes increased for several days after the onset and peaked on May 15.

The co-eruption tremor during the initial eruption from May 10 to 15 reached amplitudes of Dr 40–80 cm^2, corresponding to a high VEI 3. This is consistent with the initial eruption column height would indicate (VEI 3–4). This value is somewhat greater than indicated by the erupted volume of the initial phase, as reported by Trusdell et al. (2005—this issue). Extrusion of the small craggy dome is constrained by visual observations to have occurred between May 20 and the first few days of June, likely around the sharp drop in LP tremor about May 24. On June 13 and 14, two explosions of VEI 2 destroyed the small craggy dome, in keeping with the erupted volume of the dome destruction (Trusdell et al., 2005—this issue).

We suspect that the initial peak in inflation, VT rates, the first small peak in LP tremor, and the lack of significant explosion signal indicate that the initial eruptive pulse was quite passive, but contained a high volume of a free vapor phase gas atop the column of magma, essentially a phreatic eruption. This would explain the surprisingly high plume height of 10–13 km and rather high SO_2 values from TOMS data (Krueger et al., 1995), both of which would seem to indicate VEI 3–4. However, the smaller erupted volume of juvenile product and low co-eruption tremor amplitude during the first day suggest a lower VEI for the initial eruption. A secondary eruptive pulse occurred approximately 12 h after the initial eruption, inferred from the second small inflation pulse and second peak in VT rate. Approximately 1 day later, a third eruption sequence occurred, as inferred from the first large peak in LP tremor and main peak in VT magnitudes. Both periods of eruptive activity after the initial onset resulted from pulses of magma rising towards the surface. We believe the two large, longer duration peaks in LP tremor about 6 and 10 days later result from the magma approaching the near surface. Magma eventually reached the surface forming a small craggy dome several days after that, agreeing with VLP event occurrence. The surface then cooled, trapping magmatic gases, which accumulated beneath that surface. A few weeks later, the dome ruptured and was destroyed by a few of small explosions.

The fortuitous seismic recording of the 2003 Anatahan eruption onset by a broadband seismograph has provided a rich data set for analysis. In addition to conventional observations of VT and LP events, the broadband seismograph recorded tilt and VLP signals associated with the initial eruption. This event represents the first time that co-eruption tilt has been determined from a portable broadband seismograph, and the tilt provides important details on the initial inflation and deflation of the edifice. Careful examination of other broadband data sets may show such tilt signals. In addition, at least four different types of VLP signals have been identified, providing a high-quality data set for further analysis. The wide variety of volcanic signals fortuitously recorded with a portable broadband seismograph suggests that further installation of broadband seismographs surrounding both active and inactive volcanoes should be extremely useful.

Acknowledgements

We thank Juan T. Camacho, Ray Chong, and Rudolph Pua of the Saipan Emergency Management Office for assistance in deploying the seismographs. We thank Captain Verlini and the crews of the R/V Wecoma and the Super Emerald, as well as Mike Cunningham for transport and logistics. We also thank Phil Dawson and Malcolm Johnston at the USGS, Menlo Park for help in understanding volcanic earthquakes and tilt. Additional gratitude is extended to Brian Shiro for artistic assistance. We also wish to thank Andy Lockhart, Jeff Marso, John Ewert, and C. Dan Miller of the USGS Volcano Disaster Assistance Team, Frank Trusdell and Stuart Koyanagi of the Hawaiian Volcano Observatory, and Dick More and Bob Tilling of the USGS for help getting the initial real-time monitoring going and helping understand the initial activity and assistance with information transfer. Instruments for this study were obtained from the PASSCAL program of IRIS (Incorporated Research Institutions in Seismology). This research was supported by the Margins program of the National Science Foundation under grant OCE0001938.

References

Almendros, J., Chouet, B.A., Dawson, P., Bond, T., 2002. Identifying elements of the plumbing system beneath Kilauea volcano, Hawaii, from the source locations of very-long-period signals. Geophysical Journal International 148, 303–312.

Arciniega-Ceballos, A., Chouet, B.A., Dawson, P., 2003. Long-period events and tremor at Popocatepetl volcano (1994–2000) and their broadband characteristics. Bulletin of Volcanology 65, 124–135.

Aster, R., et al., 2003. Very long period oscillations of Mount Erebus Volcano. Journal of Geophysical Research 108 (B11), 2,522.

Banks, N., Ewert, J., 1990. Volcanic activity report. Bulletin of the Global Volcanism Network 15 (03).

Battaglia, J., Aki, K., Montagner, J.-P., 2000. Tilt signals derived from a GEOSCOPE VBB station on the Piton de la Fournaise volcano. Geophysical Research Letters 27 (5), 605–608.

Chouet, B.A., 1996. Long-period volcano seismicity: its source and use in eruption forecasting. Nature 380, 309–316.

Chouet, B.A., 2003. Volcano seismology. Pure and Applied Geophysics 160, 739–788.

Chouet, B.A., et al., 2003. Source mechanisms of explosions at Stromboli Volcano, Italy, determined from moment–tensor inversions of very-long-period data. Journal of Geophysical Research 108 (B1), 2019–2043.

Guffanti, M., Ewert, J.W., Gallina, G.M., Bluth, G.J.S., Swanson, G.L., 2005. Volcanic-ash hazard to aviation during the 20032004 eruptive activity of Anatahan volcano, Commonwealth of the Northern Mariana Islands. Journal of Volcanology and Geothermal Research 146, 241–255 (this issue).

Harlow, D.H., et al., 1996. Precursory seismicity and forecasting of the June 15, 1991, eruption of Mount Pinatubo. In: C.G. Newhall, R.S. Punongbayan (Eds.), Fire and mud: eruptions and lahars of Mount Pinatubo, Philippines. Philippine Institute of Volcanology and Seismology, Quezon City, and the University of Washington Press, Seattle and London, pp. 285–306.

Koyanagi, R., Chong, R., 1993. Volcanic activity report. Bulletin of the Global Volcanism Network 18 (05).

Krueger, A.J., et al., 1995. Volcanic sulfur dioxide measurements from the total ozone mapping spectrometer instruments. Journal of Geophysical Research 100, 14057–14076.

Lahr, J.C., Chouet, B.A., Stephens, C.D., Power, J.A., 1994. Earthquake classification, location, and error analysis in a volcanic environment: implications for the magmatic system of the 1989–1990 eruptions of Redoubt volcano, Alaska. Journal of Volcanology and Geothermal Research 62, 137–151.

Legrand, D., et al., 2002. Stress tensor analysis of the 1998–1999 tectonic earthquake swarm of northern Quito related to the volcanic swarm of Guagua Pichincha volcano, Ecuador. Tectonophysics 344, 15–36.

Makhoul, J., 1975. Linear prediction: a tutorial review. Proceedings of the IEEE 63 (4).

McNutt, S.R., 1994. Volcanic tremor amplitude correlated with the volcano explosivity index and its potential use in determining ash hazards to aviation. Acta Vulcanologia 5, 193–196.

Ohminato, T., Chouet, B.A., Dawson, P., Kedar, S., 1998. Waveform inversion of very long period impulsive signals associated with magmatic injection beneath Kilauea Volcano, Hawaii. Journal of Geophysical Research 103 (B10), 23839–23862.

Pallister, J.S., Trusdell, F.A., Brownfield, I.K., Siems, D.F., Budahn, J.R., Sutley, S.F., 2005. The 2003 phreatomagmatic eruptions of Anatahan volcanotextural and petrologic features of deposits at an emergent island volcano. Journal of Volcanology and Geothermal Research 146, 208–225 (this issue).

Rodgers, P.W., 1968. The response of the horizontal pendulum seismometer to Rayleigh and Love waves, tilt, and free oscillations of the earth. Bulletin of the Seismological Society of America 58, 1384–1406.

Rowe, C.A., Thurber, C.H., White, R.A., 2004. Dome growth behavior at Soufriere Hills Volcano, Montserrat, revealed by relocation of volcanic event swarms, 1995–1996. Journal of Volcanology and Geothermal Research 134, 199–221.

Sasamoto, F., et al., 1990. Volcanic activity report. Bulletin of the Global Volcanism Network 15 (04).

Suyehiro, K., et al., 1996. Continental crust, crustal underplating, and low-Q upper mantle beneath and oceanic island arc. Science 272, 390–392.

Trusdell, F.A., Moore, R.B., Sako, M., White, R.A., Koyanagi, S.K., Chong, R., Camacho, J.T., 2005. The 2003 eruption of Anatahan Volcano, Commonwealth of the Northern Mariana Islands: chronology, volcanology, and deformation. Journal of Volcanology and Geothermal Research 146, 184–207 (this issue).

Watanabe, T., Tabei, T., Matsushima, T., Kato, T., Nakada, S., Yoshimoto, M., Chong, R., Camacho, J.T., 2005. Geodetic constraints for the mechanism of Anatahan eruption of May 2003. Journal of Volcanology and Geothermal Research 146, 77–85 (this issue).

White, R.A., Power, J.A., 2001. Distal volcano-tectonic earthquakes: diagnosis and use in eruption forecasting. EOS Transactions-AGU 82 (47) (Abstract #U32A-0001).

White, R.A., et al., in preparation. Seismicity associated with the 2004 Anatahan eruption sequence.

Wielandt, E., Forbriger, T., 1999. Near-field seismic displacement and tilt associated with the explosive activity of Stromboli. Annali di Geofisica 42, 407–416.

Wiens, D.A., et al., 2004. Observing the historic eruption of Northern Mariana Islands Volcano. EOS Transactions-AGU 85, 2–4.

Wiens, D.A., et al., submitted for publication. Tilt recorded by a portable broadband seismograph: The 2003 eruption of Anatahan Volcano, Mariana Islands. Geophysical Research Letters (May 2005).